

Herbal Extract Loaded Chitosan-Based Nanofibers as a Potential Wound-Dressing

Esmaeil Mirzaei^{1, 2}, Saeed Sarkar², Seyed Mahdi Rezayat², Reza Faridi-Majidi^{2*}

¹Department of Medical Nanotechnology, School of Advanced Medical Sciences and Technologies, Shiraz University of Medical Sciences, Shiraz, Iran

²Department of Medical Nanotechnology, School of Advanced Technologies in Medicine, Tehran University of Medical Sciences, Tehran, Iran

Use your device to scan and read the article online



Abstract

*Corresponding author:
Reza Faridi-Majidi
Department of Medical Nanotechnology, School of Advanced Technologies in Medicine, Tehran University of Medical Sciences, Tehran, Iran
refaridi@sina.tums.ac.ir

Received: 13.03.2016
Revised: 30.03.2016
Accepted: 02.04.2016

Key words: electrospinning, Nanofiber, Chitosan, Melilotus officinalis extract.

Semelil is an herbal-based compound which is used for the treatment of chronic wounds, especially diabetic foot ulcers. On the other hand, Electrospun nanofibers have many characteristics such as mimicking extracellular matrix structure, efficiency as bacterial barrier, appropriate water vapor transmission rate, and provision of adequate gaseous exchange which make them ideal candidates for wound-healing application. The aim of this study was to incorporate Semelil in electrospun nanofibers to benefit both the advantages of Semelil and electrospun nanofibers for the treatment of wounds. To this aim, the blend solution of chitosan, polyethylene oxide (PEO) and the herbal extract were electrospun and chitosan-based nanofibers loaded with the herbal extract were fabricated. The as-spun fibers were characterized by scanning electron microscopy (SEM), Fourier transform infrared spectroscopy (FTIR) and thermogravimetric analysis (TGA). The swelling ratio and drug release behavior of the electrospun fibers were also studied. Uniform and bead-free nanofibrous mats loaded with 10-50 Wt. %extract were successfully fabricated. The FTIR spectrum indicated that the chemical nature of chitosan was not changed in the process of electrospinning. TGA analysis confirm both polymers and extract in electrospun mats. The extract loaded mats showed a high swelling ratio and a burst release of extract after 1h incubation in PBS. Mats with lower amount of drug exhibited graduate increase in the cumulative release of drug after initial burst release.

 <https://doi.org/10.18869/nrip.jamsat.2.1.141>

Introduction

Diabetes is the most common metabolic disease worldwide and foot ulcers are one of the main complications in diabetes mellitus. Many different methods have been proposed to accelerate wound-healing. These treatments other than standard therapy include local use of epidermal growth factor, vacuum compression therapy, hyperbaric oxygen and peripheral stem

cell injection. A novel drug to treat such a challenging complication is a herbal extract, ANGIPARS™, which has been studied in all steps of clinical trial. This new treatment by topical and oral routs has had beneficial effects in the treatment of diabetic foot ulcer after one month (1).

Melilotus officinalis extract is the major ingredient of a modified herbal based compound, Semelil (ANGIPARS™), which is a promising candidate drug

for wound-healing(2). Results of clinical trials showed that the new herbal extract, ANGIPARS™, is very effective for treatment of foot ulcers and authors suggest that this novel drug can be superior to other treatments and can be used in all types of ulcers. Experimental studies also show no chronic or acute toxicity for ANGIPARS™ (1). The commercial product, ANGIPARS™, provides Melilotus officinalis extract in oral (capsule) and topical form (3% cream) for treatment of wounds.

On the other hand, Electrospun nanofibers have many characteristics making them ideal candidates for wound-healing application (3). Electrospun nanofibers meet many characteristics of ideal wound dressing including efficiency as bacterial barrier, absorption of excess exudates (wound fluid), provision and maintenance of a moist environment, or appropriate water vapor transmission rate, provision of adequate gaseous exchange, ability to conform to the contour of the wound area, functional adhesion, i.e., adherent to healthy tissue but non-adherent to wound tissue, and painless to patient and ease of removal (3).

The high surface area to volume ratio of electrospun nanofibers facilitate oxygen permeability and allow fluid accumulation, which are highly desirable in the wound-healing course. The pores in non-woven form of electrospun scaffolds (normally 1–10 µm) are small enough to prevent bacterial penetration (4). Meanwhile, nano scale fibers that impart the dressing with small interstices and high effective surface area can promote hemostasis. Such function of hemostasis is activated from the physical feature of the nanofibrous dressings without using a haemostatic agent (3).

In addition, therapeutic agents can be incorporated into electrospun nanofibers to give them additional benefits for wound dressing applications. Antibiotics, growth factors, and anesthetic are some therapeutic agents incorporated in electrospun nanofibers used as wound dressing. Meanwhile, the controlled release of therapeutics from electrospun nanofibers is another benefit of electrospun nanofibers as wound dressing (5).

A wide range of natural and synthetic polymers can be electrospun into nanofiber matrices with structural integrity and specific fiber arrangements (6). Polymers used in electrospun membranes as wound dressing include collagen, gelatin, fibrinogen, chitosan, polyurethane, polycaprolactone (PCL), polylactic acid (PLA), and

poly (lactic-co-glycolic) acid(PLGA), or some blends of the above (4,7).

Among these, chitosan has attracted many interests especially for biomedical applications because of its unique properties. Chitosan has good biocompatibility and biodegradability as well as various biological functionalities including antithrombogenic, hemostatic, and wound-healing properties(6). Chitosan-based electrospun nanofibers have shown potential for many biomedical applications owing to their structural similarity to glycosaminoglycans, a component of extra cellular matrix (ECM), and morphological proximity to fibrous collagen structures in the ECM at the scale of nanometers (50–500 nm in diameter) (6,8).

This study aimed to incorporate Melilotus officinalis extract into chitosan based nanofibers to meet both advantage of an effective herbal extract and electrospun chitosan nanofibers to provide a potential wound dressing which could accelerate wound-healing. Chitosan nanofibrous mats loaded with different amounts of the extract (10, 30, 50 and 70 % by weight) were successfully prepared through electrospinning. The effects of polymer to extract ratio, applied voltage and working distance were studied on morphology and diameter of obtained nanofibers. The chemical composition, water absorption capacity and drug release behavior of the electrospun mats were also investigated.

Materials and Method

-Materials

Chitosan (CS) (low molecular weight, degree of deacetylation 91.2 %) was purchased from Easter Groups (Dong Chen) Co., Ltd, China. Polyethylene oxide (PEO) (MW 900KD) was purchased from Acros Organics. Glacial acetic acid was purchased from Merck and Melilotus officinalis extract was obtained from Rose Pharmed Co. (Iran).

-Preparation of electrospinning solutions

chitosan (3.0 Wt. %) and PEO (3.0 Wt. %) solutions were prepared separately by dissolving chitosan and PEO powder in aqueous acetic acid (90 V/V %) under magnetic stirring at 37 °C for 24 h. The obtained solutions were then mixed together

in weight ratio of CS/PEO, 90:10, as the required polymer solution for electrospinning with 3.0 Wt. % of total solid. Melilotus officinalis extract dissolved in 90% (v/v) aqueous acetic acid for 20% (w/w) concentration and then add to Chitosan/PEO blend solution (polymer solution) to obtain polymer/extract solution with polymer to extract weight ratio of 100:0, 90: 10, 70: 30, 50:50 and 30: 70 (Table 1).

| Chitosan/PEO weight ratio | Acetic acid concentration | Polymer /extract weight ratio | Nanofibers morphology | Diameter±S D (nm) |
|---------------------------|---------------------------|-------------------------------|-------------------------------|-------------------|
| 90: 10 | 90 | 100: 0 | Uniform, Bead free nanofibers | 288±60 |
| 90: 10 | 90 | 90: 10 | Uniform, Bead free nanofibers | 292±68 |
| 90: 10 | 90 | 70: 30 | Uniform, Bead free nanofibers | 331±74 |
| 90: 10 | 90 | 50: 50 | Uniform, Bead free nanofibers | 442±116 |
| 90: 10 | 90 | 30: 70 | No distinct nanofibers | - |

Table 1. Preparation of CS/PEO nanofibers loaded with different amount of Melilotus officinalis extract.

-Electrospinning

The electrospinning processes were carried out using Electraris (FNM, Tehran, Iran). To produce extract loaded CS/PEO nanofibrous mats, the polymer solutions with different amounts of the extract (Table 1) was placed into a 5 ml plastic syringe with a blunt-ended 18-G stainless steel needle. An aluminum foil was wrapped on the Electraris rotating drum as collector and was located at the distance of 17 cm from the needle.

-Characterization of nanofibers

The size and morphology of produced nanofibrous mats were analyzed using scanning electron microscopy (SEM) (Philips XL30). A small section of each nanofibrous mat was sputtered with a thin layer of gold and then analyzed by SEM.

Fourier transform infrared spectroscopy (FTIR) measurements were performed (Perkin-Elmer) by the KBr method.

A syringe pump fed the solution to the needle tip at the injection rate of 1.0 ml/h. The wire of a DC positive high voltage was connected to the metallic needle and the collector to the ground. The applied voltage, and drum speed were fixed at 20 kV and 200 rpm, respectively.

Furthermore, the effects of applied voltage and working distance on morphology and diameter of 30 Wt. % extract loaded nanofibers were investigated when others parameters were kept constant.

The compositional analysis of the fiber mats was done using a (TGAQ50 TA Instruments) thermo gravimetric analyzer (TGA). Samples were weighed and heated at 20 °C/min from 40 °C to 600 °C and the degradation peaks and unburned material residue were obtained for each sample.

The swelling degree of electrospun mats was determined by a gravimetric method. The electrospun mats were immersed in phosphate buffered saline, PBS (pH=7.4), at room temperature for 24 h. The samples were then

taken out, the excess surface water was removed by filter paper, and the swelled mats were weighed.

$$\text{swelling ratio (\%)} = \frac{W_s - W_0}{W_0} \times 100$$

where W_s denotes the weight of the swelled mat and W_0 denotes the weight of the mat in its dry state after 24 h immersing in PBS.

The swelling ratio was measured as following equation:

-Extract release profile evaluation

UV-Visible absorbance of total flavonoid in buffer was considered as an indicator to evaluate the extract release profile of the electrospun mats. The dried, electrospun, extract-loaded, nanofibrous mats were first sectioned into 12×12 cm² squares and the extract content was determined as a function of mat weight.

The samples were placed into individual vials containing 50 ml phosphate buffer saline (pH=7.4) and the vials were incubated at 37 °C. At specified time intervals, 5 ml of the buffer was withdrawn and replenished with an identical volume of fresh buffer. The solution of 1.8 ml distilled water, 3 ml

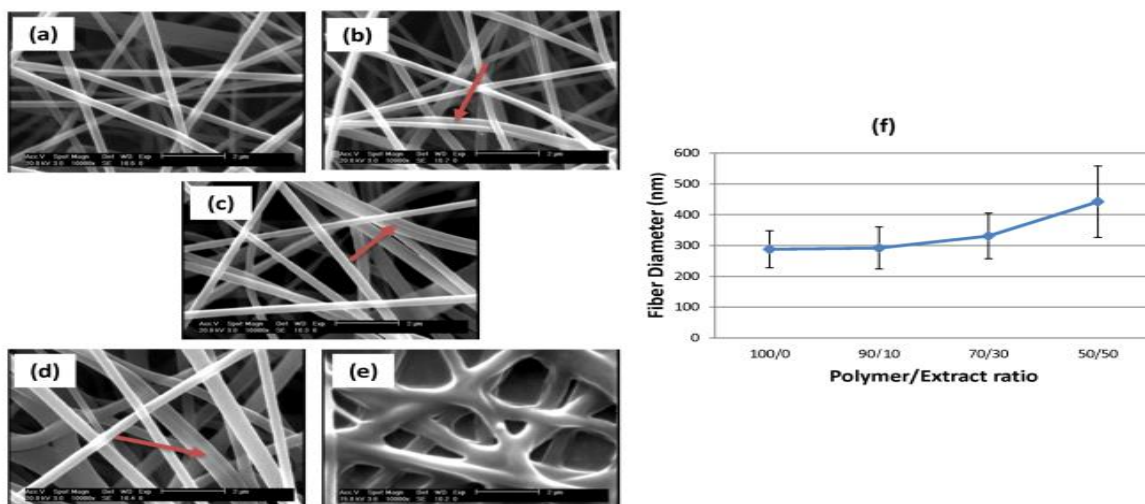


Figure 1. Scanning electron micrographs of electrospun CS/PEO nanofibers loaded with different amounts of Melilotus officinalis extract: (a) 0 % (polymer/extract 100: 0), (b) 10 % (polymer/extract 90: 10), (c) 30 % (polymer/extract 70: 30), (d) 50 % (polymer/extract 50: 50) and (e) 70 % (polymer/extract 30: 70). (f) Shows nanofibers mean diameter vs polymer/extract ratio.

methanol, 0.10 ml aluminum chloride (10 % v/v) and 0.10 ml potassium acetate (1M) was prepared and then added to the each withdrawn buffer to read the total flavonoid absorbance by UV-Visible spectroscopy at 415 nm wavelength. A standard

calibration plot was used to determine the concentration of the released extract. The percentage of the released extract was then calculated based on the initial weight of the extract incorporated in the electrospun mats.

Results and discussion

-Electrospun *Melilotus officinalis* extract loaded nanofibers

Chitosan based nanofibers incorporated with various amounts of the *Melilotus officinalis* extract were fabricated by electrospinning under condition described in the method section. The morphology of the nanofibers was investigated by scanning electron microscopy. The SEM images of CS/PEO (90:10 weight ratio) nanofibers incorporated with different amounts of *Melilotus officinalis* extract are shown in Fig 1. As illustrated in this figure the CS/PEO mat had uniform, bead-free and randomly oriented nanofibrous structure. Incorporation of *Melilotus officinalis* extract to CS/PEO nanofibers up to 50 % (polymer/extract 50: 50) had also lead to uniform and bead-free nanofibrous structure. However, some lateral adjacent were observed for some nanofibers which indicated in Fig. 1 by arrows. Incorporation of 70 % extract to CS/PEO nanofibers (polymer/extract 30: 70) did not lead to fine and distinct nanofibers (Fig. 1e).

Average fiber diameter size was determined by averaging the diameter of 30 random fibers; the smallest and largest diameter measurement were included in this average. Average fiber diameter (Fig. 1f, Table 1) increased as the ratio of *Melilotus officinalis* extract to polymer was increased. The CS/PEO nanofibers had the diameter of 288 ± 60 nm. By incorporating the extract into the CS/PEO nanofibers an increase in nanofibers diameter were observed. The 10 % extract loaded nanofibers (polymer/extract 90: 10) had diameter of 292 ± 68 nm. The nanofibers diameter increase to 331 ± 74 and 442 ± 116 nm for 30 % (polymer/extract 70:30) and 50 % (polymer/extract 50:50) extract loaded nanofibers, respectively.

Addition of drug molecules into electrospinning polymer solution may affect the final fiber diameter by changing the solution parameters such as viscosity or conductivity (9-11). Fibers diameter increase when the viscosity increase or conductivity decreases. By decreasing the viscosity of polymer solution the polymer chain entanglement increase and so causes higher resistance of polymer solution to be stretched by charges on the jet and thus making bigger fibers diameter(12). Another effect of increasing viscosity is decreasing jet instability, which in turn decrease jet path from needle to collector. This decreased jet path means that there is less stretching on polymer jet which results in larger fibers diameter (13). In the other hand, decreasing solution conductivity also leads to increase in fibers diameter. Decreasing solution

conductivity leads to decreases in the charge density of the polymer jet and subsequently less stretching on the jet which results in larger fibers diameter(14,15). In this study, incorporation of *Melilotus officinalis* extract into chitosan solution lead to increasing in diameter of resulted electrospun fibers. This increase can attribute to either increasing viscosity or decreasing conductivity of solution.

As shown in Figure 2 for all voltages, uniform and bead-free nanofibers were formed. The average diameter of fibers was decreased by increasing the applied voltage (Fig. 2e). The average diameter decrease from 409 ± 39 to 321 ± 70 nm by increasing voltage from 10 to 25 kV.

- Effects of applied voltage and working distance on fibers morphology

The effects of applied voltage on morphology and diameter of nanofibers loaded with 30 Wt. % extract (polymer/extract 70:30) were investigated when the other parameters including working distance and injection rate were fixed at 17 cm and 1 ml/h, respectively. The applied voltage varied from 10-25 kV. The SEM images of obtained nanofibers at 10, 15, 20 and 25 kV applied.

According to the literature, increasing applied voltage can increase fibers diameter by two mechanisms. Higher voltage accelerates stretching of the polymer solution because of greater columbic forces in the jet as well as stronger electrostatic field. These then lead to production of smaller fibers diameter (16). Higher voltage also facilitates formation of secondary jets which in turn can reduce fibers diameter (17).

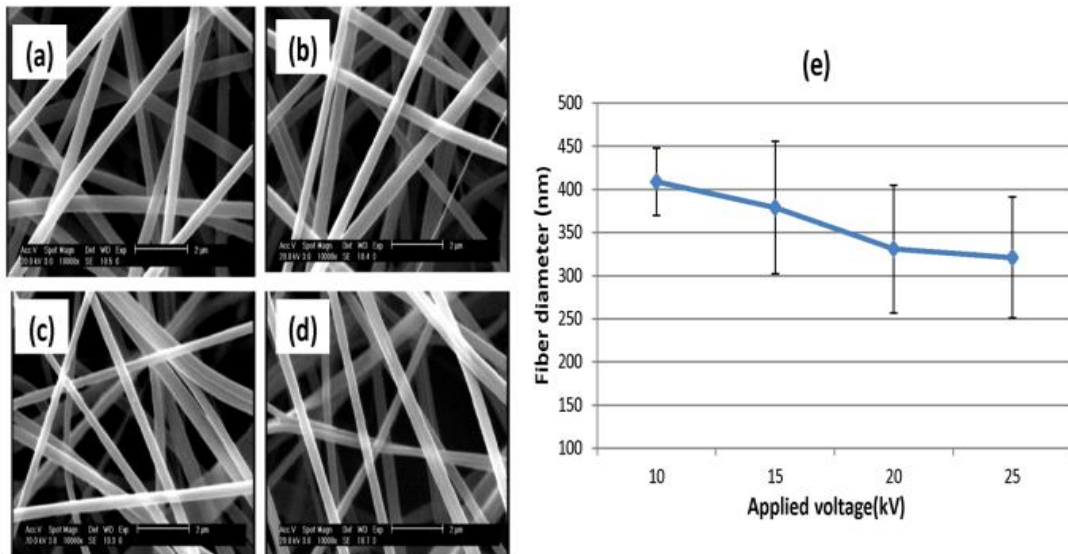


Figure 2. Scanning electron micrographs of 30 Wt. % loaded extract electrospun fibers at different applied voltage (kV): (a) 10, (b) 15, (c) 20 and (d) 25. (e) Shows nanofibers mean diameter vs applied voltage

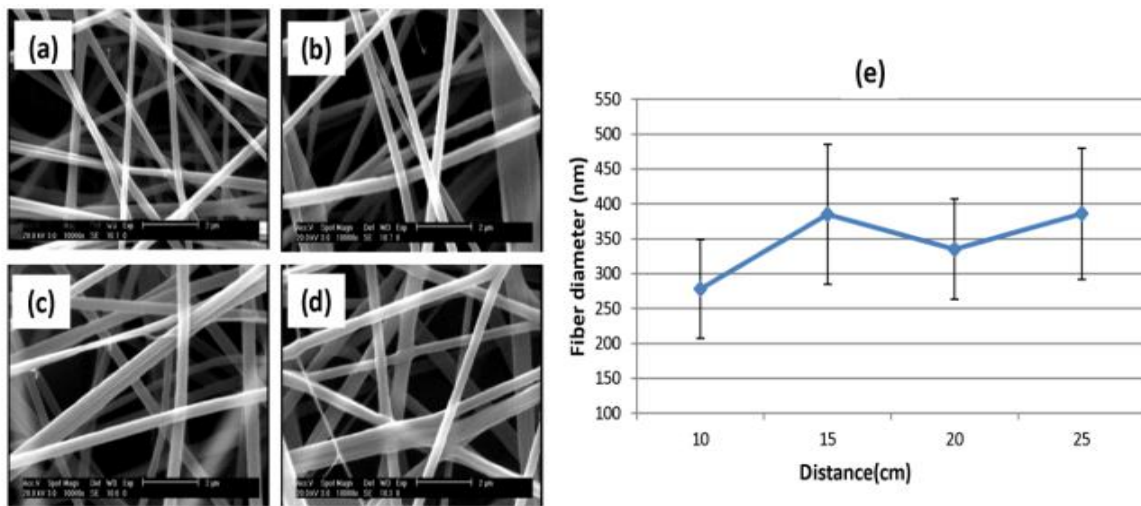


Figure 3. Scanning electron micrographs of 30 Wt. % loaded extract electrospun fibers at different working distance (cm): (a) 10, (b) 15, (c) 20 and (d) 25. (e) Shows nanofibers mean diameter vs. working distance.

By fixing applied voltage at 20 kV the effects of working distance on 30 Wt. % extract (polymer/extract 70:30) nanofibers were

investigated. Fig. 3 represents the SEM images of nanofibers at distance of 10, 15, 20 and 25 cm.

Uniform and bead-free nanofibers obtained for all distance. The effect of working distance on the nanofibers diameter is however contradictory, the distance increase from 10 to 15 cm, the diameter increase from 278 ± 71 to 358 ± 100 nm. By increasing distance to 20 cm, the diameter decrease to 335 ± 72 nm while an increase indistance to 25 cm again decreased the diameter to 386 ± 96 nm.

However, there are cases where at a longer distance, the fiber diameter increases. This is due to the decrease in the electrostatic field strength resulting in less stretching of the fibers(21).

fibers mean diameter changed by increasing distance but not in a regular manner. When

According to the literature, increasing distance can decrease or increase fibers diameter(18). In general, increasing the distance results in a decrease in the average fiber diameter(19). The longer distance means that there is a longer flight time for the solution to be stretched before it is deposited on the collector (20).

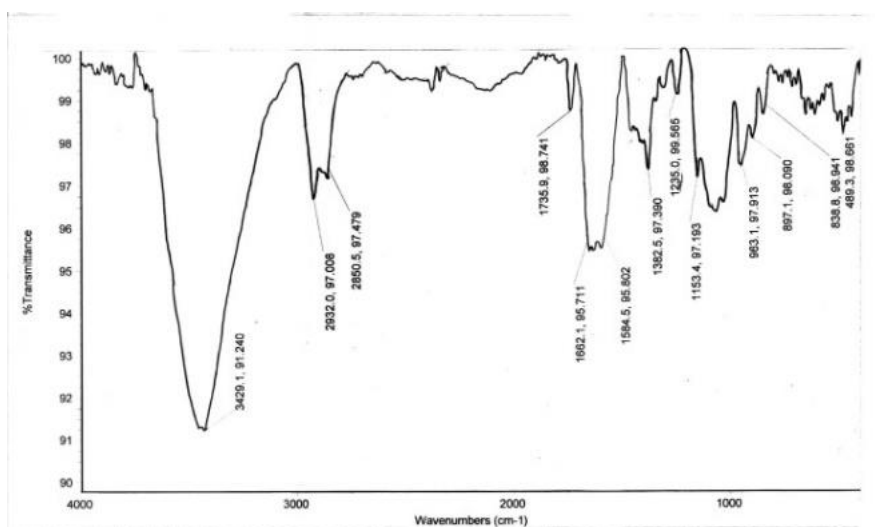


Figure 4. FTIR spectra of CS/PEO nanofibers

-Characterization of electrospun nanofibers

To investigate the chemical structure of chitosan based electrospun nanofibers, The FTIR analysis of chitosan/PEO nanofibers was carried out as shown in Fig 4.

The FTIR spectrum of electrospun CS/PEO (90: 10) nanofibers showed the characteristic absorbance bands of chitosan. The main bands in the FTIR spectrum of chitosan can be seen as follows: The intense band around 3430 cm^{-1} should be assigned to OH and NH stretch. Two middle strong bands at 1662 and 1584 cm^{-1} for amide I and amide II. The absorption bands at 1154 cm^{-1} assign to anti-symmetric stretching of the C-O-C bridge. Two weak bands at 2932 and 2850 cm^{-1} corresponds to CH stretch and the peak at 1382 cm^{-1} assign to deformation of C-CH₃(22,23).The

FTIR spectrum also indicated that the chemical nature of chitosan was not changed in the process of electrospinning.

Compositional analysis was done using TGA. The TGA curve of pure chitosan powder, pure PEO powder, CS/PEO (90: 10) nanofibers, chitosan/PEO nanofibers loaded with 10 and 30 % Wt. % Melilotus officinalis extract, and Melilotus officinalis extract are showed in Fig 5.

Decomposition temperature(s) and residual amounts at $600\text{ }^{\circ}\text{C}$ derived from TGA cures are indicated in Table 2. TGA analysis of the CS/PEO fibers (Fig 5a) confirmed the presence of both the polymer fractions in the blend. Pure chitosan was found to thermally decompose at $\sim 306\text{ }^{\circ}\text{C}$ and pure PEO shows degradation peaks at $\sim 402\text{ }^{\circ}\text{C}$. Degradation peaks for CS/PEO nanofibers were at 113 , 286 and $386\text{ }^{\circ}\text{C}$. The unburnt residue material

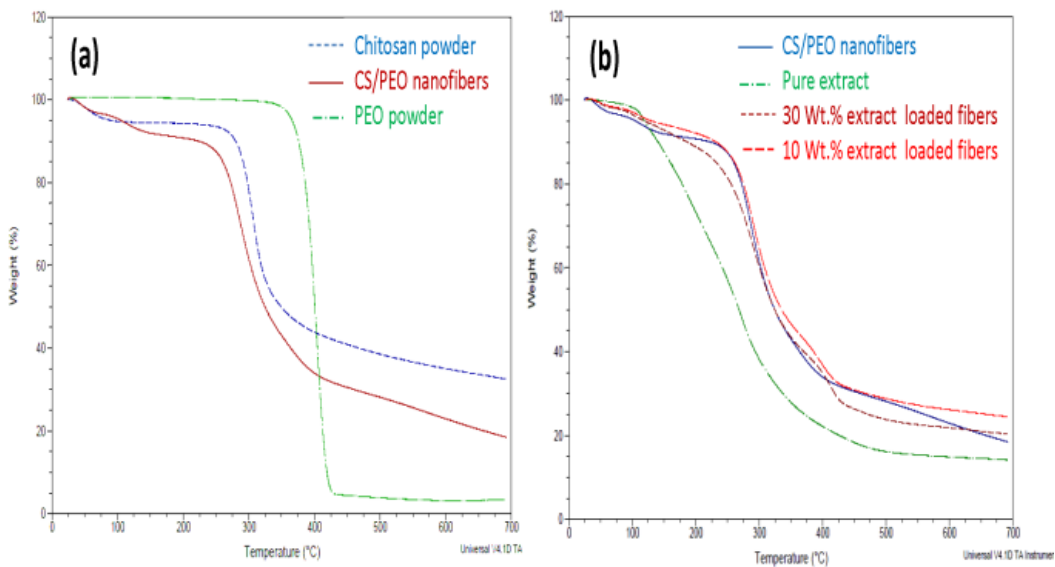


Figure5. TGA analysis of CS, PEO, Melilotus officinalis extract and electrospun nanofibers.

| Sample | Decomposition temperature (°C) | Residual in 600 °C (%) |
|---------------------------------------|-----------------------------------|------------------------|
| Pure chitosan powder | 306 | 33 |
| Pure PEO powder | 402 | 3 |
| CS/PEO (90: 10) nanofibers | 113,286,386 | 18.5 |
| Pure extract | 118, 151, 254, 273, 285, 311, 438 | 14 |
| 30 % extract loaded CS/PEO nanofibers | 105, 154, 288, 409, 446, 463 | 20 |
| 10 % extract loaded CS/PEO nanofibers | 110, 288, 378 | 24.5 |

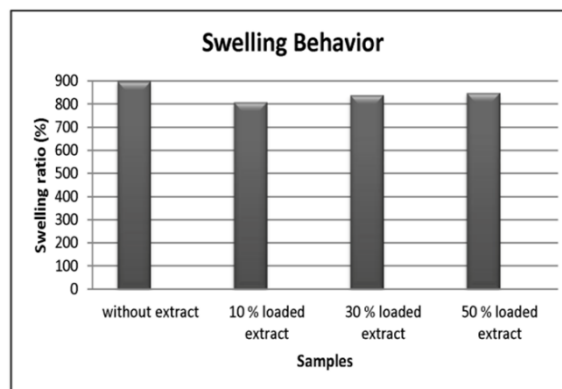


Figure6. Swelling behavior of CS/PEO nanofibers loaded with different amounts of Melilotus officinalis extract.

Table 2. Thermal properties of polymers and electrospun polymer blends

for Pure chitosan, pure PEO and CS/PEO nanofibers was 33%, 3% and 18%, respectively.

TGA analysis of the extract and extract loaded nanofibers (10 and 30 Wt.%) confirmed the

-Swelling behavior

To investigate the water absorption capability of chitosan based nanofibers, the swelling behavior of nanofibers was studied. The more swelling ratio (%) related to the more water absorption capability. The swelling ratio (%) of electrospun mats is stated in Fig 6. It can be seen that the swelling ratio of CS/PEO mats did not decrease significantly by incorporating different amounts Melilotus officinalis extract. In fact, all samples showed high swelling ratio between 800-900 %, which indicate high water absorption capability of chitosan based nanofibers.

Cumulative release profile of the extract from the varying electrospun chitosan based mats are stated in Fig. 7. These samples involve 10 Wt. %, 30 Wt. % and 50 Wt. % extract loaded nanofibrous mats. All mats show a quick burst of extract release in the first hour, however the initial amount of the released drug was found to vary as a function of extract concentration. For example, the mats with 10 Wt. % extract exhibited 26 % release at the first hour while the 30 and 50 Wt. % loaded mats released about 44 % in the same hour. It also should be noted that the mats with the lower amount of extract (i.e., 10 Wt. % loaded extract mat) showed a sustained release profile after the initial burst. The cumulative amount of the released extract for this sample reached to maximum of 40 % after 8h (about 14% of the extract was released continuously over 7h). However, the mats with higher amounts of extract (i.e., 30 Wt. % and 50 Wt. %) reached to maximum release of about 48-50 % after 3h (about 4 % release over 2h). this behavior can explain as described below.

The burst effect in the initial stages could be due to the release of drug entrapped on the surface of nanofibers. During electrospinning, if there are limited physical interactions between the drug and the polymer matrix, then the majority of the drug will

presence of both the polymers and the extract in the nanofibers (Fig 5b). The degradation peaks and residual percent of the extract and extract loaded nanofibers are shown in Table 2.

likely be localized on the surface of the nanofibers. In such an arrangement, the drug molecules on the fiber surface can be easily washed away in aqueous solutions, thus resulting in a large initial burst at short times and minimum sustained release at longer times(11). Here, Hydrophilic nature of chitosan backbone may lead to low physical interaction with water insoluble extract and subsequently placement of the extract on the surface of nanofibers. High swelling ratio of chitosan based mats is probably another reason for burst release of extract from the mats. As indicate in Fig 6 all chitosan based mats showed high swelling ratio. High swelling ratio may facilitate the extract diffusion from the polymer surface and matrix.

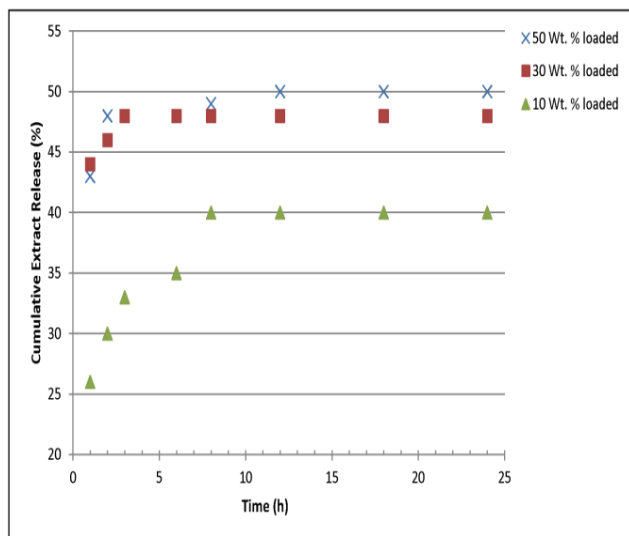


Figure7. Cumulative release profile of Melilotus officinalis extract from the nanofibrous mats incorporated with various concentrations of extract in PBS (pH=7.4).

Conclusion

Chitosan-based nanofibrous mats loaded with *Melilotus Officinalis* extract were fabricated successfully via electrospinning. Such mats promise an effective wound dressing especially for

the treatment of chronic ulcers through modulating advantage of chitosan electrospun nanofibrous mat and an effective herbal drug (*Semellil* extract).

References

1. Larijani B, Hasani Ranjbar S. OVERVIEW OF DIABETIC FOOT; NOVEL TREATMENTS IN DIABETIC FOOT ULCER. *DURO*. 2008;16(1):1-6.
2. Khorram Khorshid HR, B S, Heshmat R, Abdollahi M, Salari P, Farzamfar B, et al. In vivo and in vitro genotoxicity studies of *Semellil* (ANGIPARSTM). *DURO*. 2008;16(1):20-4.
3. Zhang Y, Lim C, Ramakrishna S, Huang Z-M. Recent development of polymer nanofibers for biomedical and biotechnological applications. *J Mater Sci Mater Med*. 2005;16(10):933-46.
4. Zhong SP, Zhang YZ, Lim CT. Tissue scaffolds for skin wound healing and dermal reconstruction. *Wiley Interdisciplinary Reviews: Nanomedicine and Nanobiotechnology*. 2010;2(5):510-25.
5. Thakur RA, Florek CA, Kohn J, Michniak BB. Electrospun nanofibrous polymeric scaffold with targeted drug release profiles for potential application as wound dressing. *Int J Pharm*. 2008;364(1):87-93.
6. Lee KY, Jeong L, Kang YO, Lee SJ, Park WH. Electrospinning of polysaccharides for regenerative medicine. *Adv Drug Del Rev*. 2009;61(12):1020-32.
7. Faghihi F, Mirzaei E, Ai J, Lotfi A, Sayahpour FA, Barough SE, et al. Differentiation potential of human chorion-derived mesenchymal stem cells into motor neuron-like cells in two-and three-dimensional culture systems. *Mol Neurobiol*. 2015:1-11.
8. Jayakumar R, Prabakaran M, Nair S, Tamura H. Novel chitin and chitosan nanofibers in biomedical applications. *Biotechnol Adv*. 2010;28(1):142-50.
9. Taepaiboon P, Rungsardthong U, Supaphol P. Vitamin-loaded electrospun cellulose acetate nanofiber mats as transdermal and dermal therapeutic agents of vitamin A acid and vitamin E. *Eur J Pharm Biopharm*. 2007;67(2):387-97.
10. Taepaiboon P, Rungsardthong U, Supaphol P. Drug-loaded electrospun mats of poly (vinyl alcohol) fibres and their release characteristics of four model drugs. *Nanotechnology*. 2006;17(9):2317.
11. Kim K, Luu YK, Chang C, Fang D, Hsiao BS, Chu B, et al. Incorporation and controlled release of a hydrophilic antibiotic using poly (lactide-co-glycolide)-based electrospun nanofibrous scaffolds. *J Controlled Release*. 2004;98(1):47-56.
12. Jarusuwannapoom T, Hongrojjanawiwat W, Jitjaicham S, Wannatong L, Nithitanakul M, Pattamaprom C, et al. Effect of solvents on electrospinnability of polystyrene solutions and morphological appearance of resulting electrospun polystyrene fibers. *Eur Polym J*. 2005;41(3):409-21.
13. Mit-upatham C, Nithitanakul M, Supaphol P. Ultrafine Electrospun Polyamide-6 Fibers: Effect of Solution Conditions on Morphology and Average Fiber Diameter. *Macromol Chem Phys*. 2004;205(17):2327-38.
14. Zong X, Kim K, Fang D, Ran S, Hsiao BS, Chu B. Structure and process relationship of electrospun bioabsorbable nanofiber membranes. *Polymer*. 2002;43(16):4403-12.
15. Choi JS, Lee SW, Jeong L, Bae S-H, Min BC, Youk JH, et al. Effect of organosoluble salts on the nanofibrous structure of electrospun poly (3-hydroxybutyrate-co-3-hydroxyvalerate). *Int J Biol Macromol*. 2004;34(4):249-56.
16. Lee JS, Choi KH, Ghim HD, Kim SS, Chun DH, Kim HY, et al. Role of molecular weight of atactic poly(vinyl alcohol) (PVA) in the structure and properties of PVA nanofabric prepared by electrospinning. *J Appl Polym Sci*. 2004;93(4):1638-46.
17. Demir MM, Yilgor I, Yilgor E, Erman B. Electrospinning of polyurethane fibers. *Polymer*. 2002;43(11):3303-9.
18. Faridi - Majidi R, Ziyadi H, Naderi N, Amani A. Use of artificial neural networks to determine parameters controlling the nanofibers diameter in electrospinning of nylon- 6, 6. *J Appl Polym Sci*. 2012;124(2):1589-97.
19. Ayutse J, Gandhi M, Sukigara S, Micklus M, Chen H-E, Ko F. Regeneration of *Bombyx mori* silk by electrospinning. Part 3: characterization of electrospun nonwoven mat. *Polymer*. 2005;46(5):1625-34.
20. Zhao S, Wu X, Wang L, Huang Y. Electrospinning of ethyl-cyanoethyl cellulose/tetrahydrofuran solutions. *J Appl Polym Sci*. 2004;91(1):242-6.
21. Lee JS, Choi KH, Ghim HD, Kim SS, Chun DH, Kim HY, et al. Role of molecular weight of atactic poly (vinyl alcohol)(PVA) in the structure and properties of PVA nanofabric prepared by electrospinning. *J Appl Polym Sci*. 2004;93(4):1638-46.
22. De Vasconcelos C, Bezerril dP, Dos Santos D, Dantas dT, Pereira M, Fonseca J. Effect of molecular weight and ionic strength on the formation of polyelectrolyte complexes based on poly (methacrylic acid) and chitosan. *Biomacromolecules*. 2006;7(4):1245-52.
23. Wan Y, Wu H, Yu A, Wen D. Biodegradable polylactide/chitosan blend membranes. *Biomacromolecules*. 2006;7(4):1362-72.
24. Barat R, Srinatha A, Pandit J, Anupurba S, Mittal N. Chitosan inserts for periodontitis: influence of drug loading, plasticizer and crosslinking on in vitro metronidazole release. *Acta Pharm*. 2007;57(4):469-77.